



# The performance of silicon detectors for the SiliPET project: A Small Animal PET Scanner based on Stacks of Silicon Detectors

**Natalia Auricchio**, Giovanni di Domenico, Guido Zavattini,  
Luciano Milano, Roberto Malaguti, Maria Ionica,  
Emanuele Fiandrini

INAF/IASFBO, Bologna (Italy) and INFN - Ferrara (Italy)  
Università di Ferrara and INFN - Ferrara (Italy)  
Università di Perugia and INFN – Perugia (Italy)

# OUTLINE

- Small animal PET scanners
- SiliPET scanner
- Monte Carlo simulation results
- Proof of principle with the MEGA detector
- Prototype detectors
- Electrical & Spectroscopic Characterization
- Spatial & Timing resolution
- Imaging Performance
- Conclusions

# Small animal PET scanners

Current small animal PET scanners are based on pixellated scintillator matrices coupled to position sensitive photomultiplier tubes with a center of mass position determination algorithm.

Scintillators are usually **high Z** and **thick** for efficiency reasons and have commonly a pixel of about 1 - 2 mm, resulting in a spatial resolution ranging from ~0.8 to 1.25 mm.

## PROBLEMS

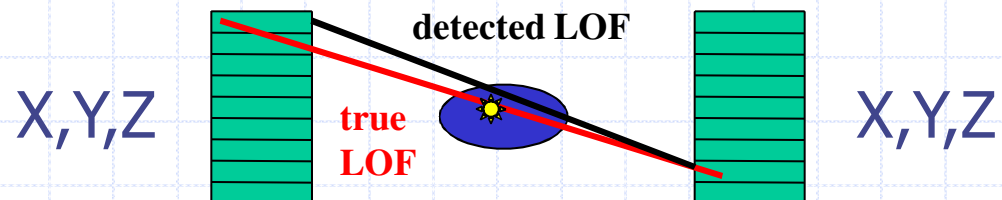
**Thickness + Lack of Depth of Interaction measurement**

PARALLAX ERROR

**High Z materials**

HIGH PHOTOFRACTION,

**BUT  $\approx 1/2$  full energy events are multiple scattered events**



# How to improve spatial resolution without loss of efficiency?

Spatial resolution degradation due to the scattering of 511 keV in small animals is negligible  $\Rightarrow$  Energy information is superfluous

A high fraction of Compton interactions in a detector of low Z materials are single interactions. In the table the interaction multiplicities are compared for two different detectors: silicon (low Z) and BGO (high Z).

Therefore different detection techniques such as solid state detectors can be used. In such cases depth of interaction can be measured and the intrinsic spatial resolution can be improved respect to high Z materials.

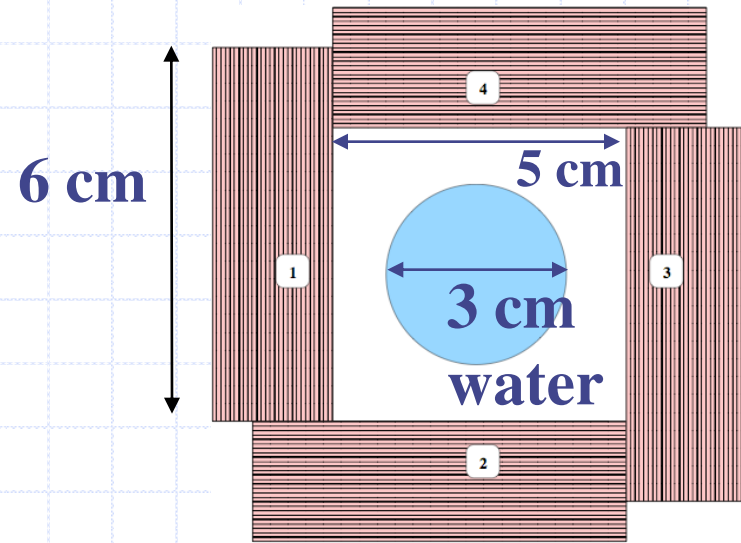
Comparison of the interactions multiplicity in Si and BGO

# interactions	% photons detected		
	<i>Si, 4cm thick</i>	<i>BGO, 1cm E&gt;350keV</i>	<i>BGO, 1cm All</i>
1	51.8	50.3	56.3
2	24.9	35.1	31.4
3	11.7	11.6	9.8
>3	11.6	3.0	2.5

$\Sigma$  interactions=49.7%

# SiliPET scanner

The small animal PET scanner proposed is based on 4 stacks of double-sided silicon detectors. Each stack is composed of 40 planar sensors with dimension  $60 \times 60 \times 1 \text{ mm}^3$  and 128 orthogonal strips on both sides to permit the measurement of the two coordinates on the plane of the detector. The third coordinate, the depth of interaction, is given by the identification of the detector plane in which the interaction takes place with a precision determined by its thickness.



The circle represents the 3 cm diameter water cylinder used to simulate the mouse body.

## Benefits:

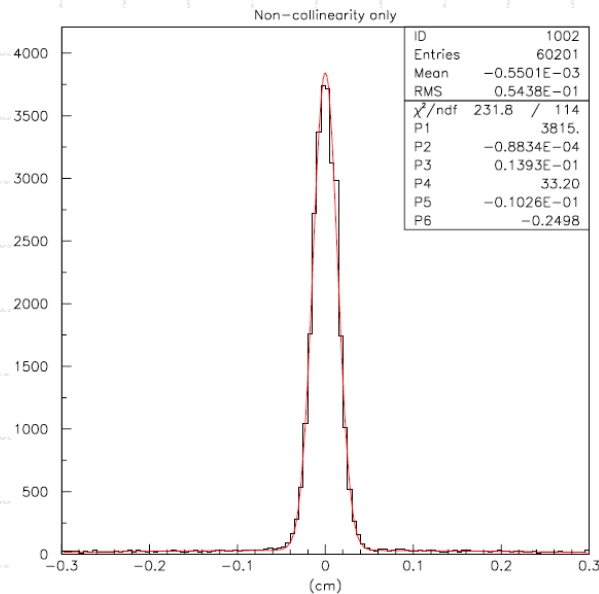
- accurate measurement of the interaction position
- measuring the depth of interaction → very compact scanner with large solid angle coverage → high sensitivity
- scanner compactness → non-collinearity effects become negligible
- no energy measurement → simplified readout electronics

**The positron range dominates the ultimate spatial resolution**

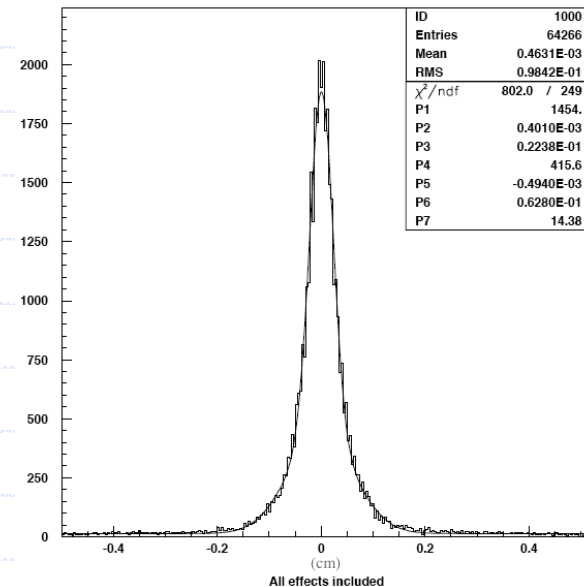
# Monte Carlo simulation results (I)

An isotropic point-like source of  $^{18}\text{F}$  is placed at the center of the system emitting positrons. Surrounding it was a 1.5 cm radius cylinder of water to simulate the positron interaction with the mouse body.

Spatial resolution: sinogram profiles

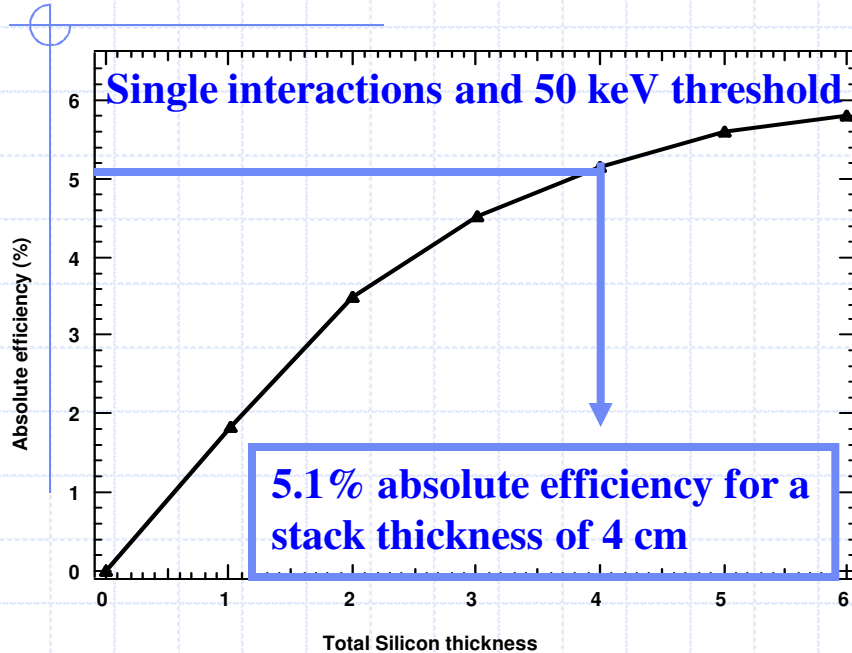


Without positron range  
FWHM = 0.33 mm (due to strip pitch)



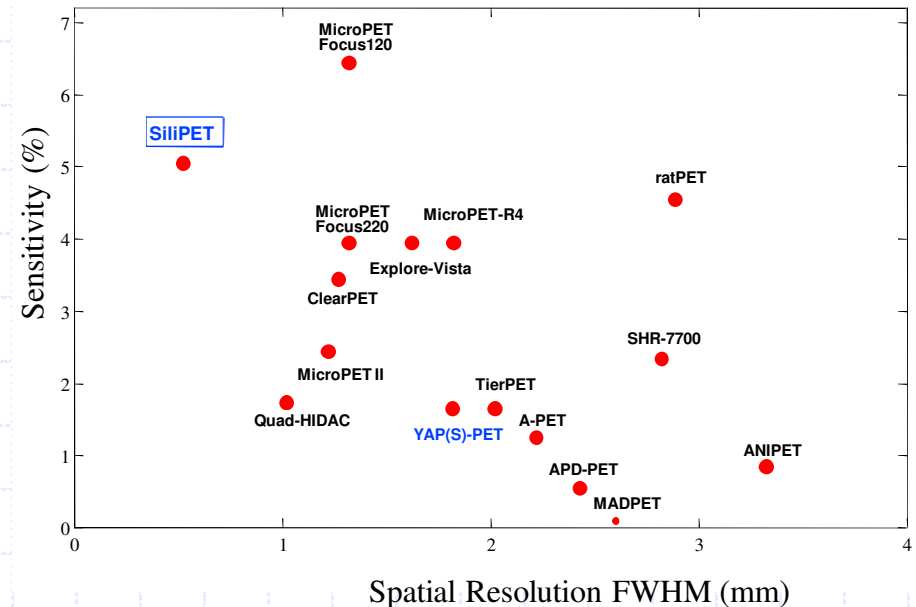
Including positron range  
FWHM = 0.52 mm

# Monte Carlo results (II)



Absolute efficiency of the scanner as a function of detector stack thickness

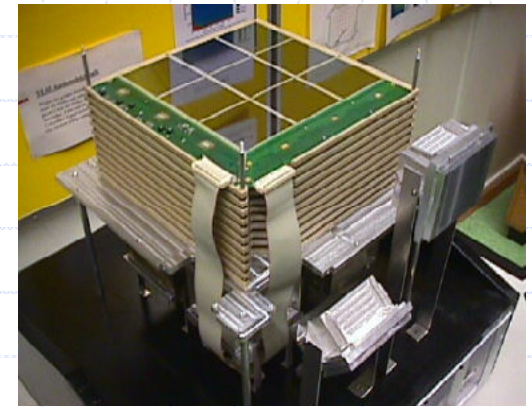
## Small Animal PET comparison





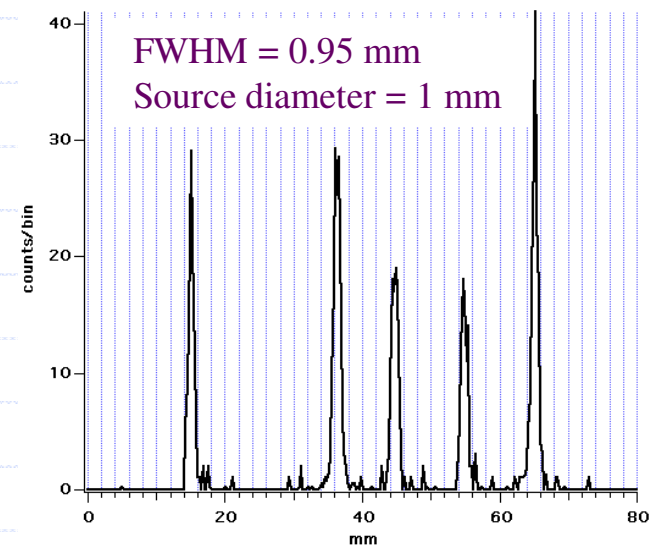
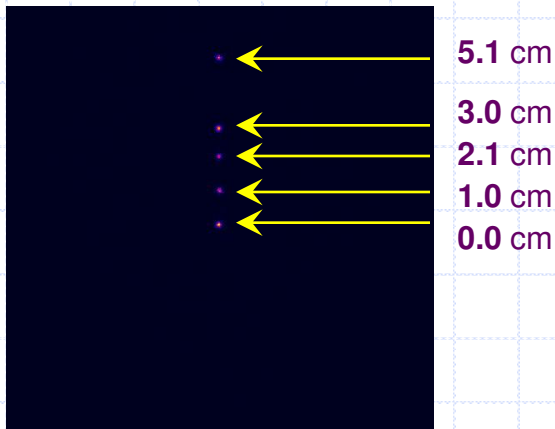
# Proof of principle with the MEGA detector

The MEGA detector was divided into two stacks 2 cm apart made of 5 and 6 prototype layers. Coincidence events between top and bottom stacks were taken, placing a small spherical  $^{22}\text{Na}$  source in 5 different positions.



MEGA prototype tracker:  
11 double sided Si detector layers ( $19 \times 19 \text{ cm}^2$ )  
Si wafer parameters:  
thickness = 0.5 mm;  
strip pitch =  $470 \mu\text{m}$

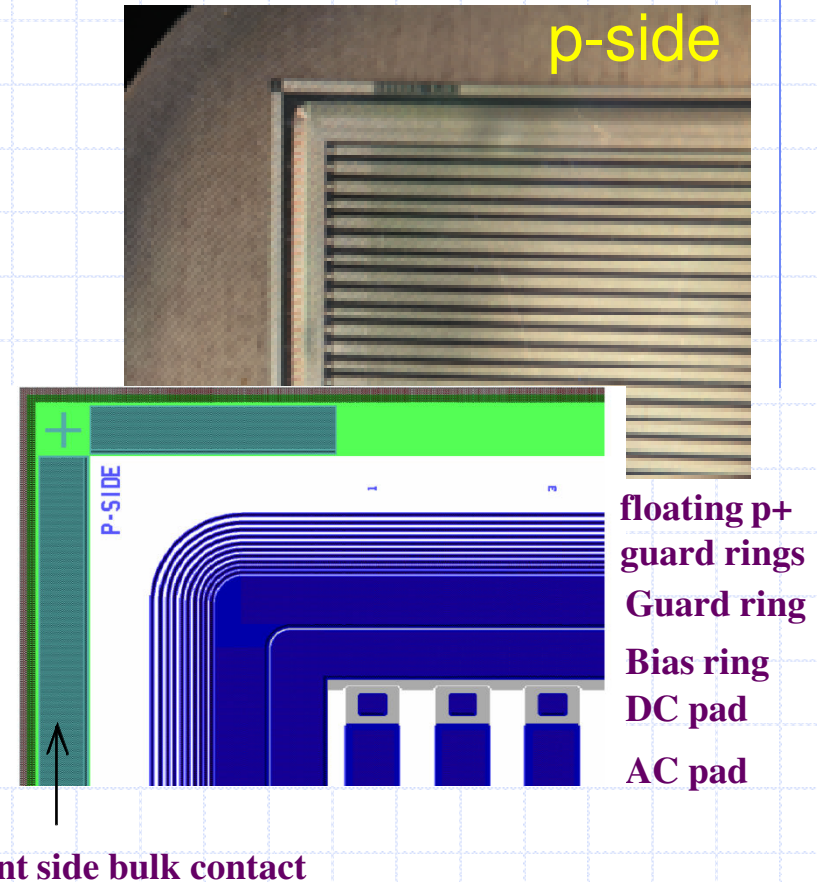
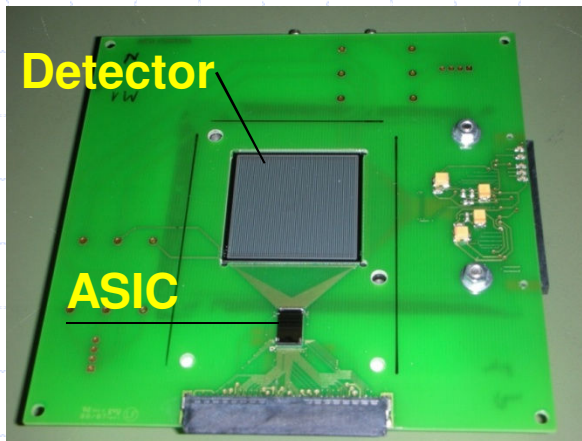
Image obtained as sum of the source in the five positions acquired (left). Profile of the reconstructed image and used to estimate the spatial resolution of the system (right).





# Prototype detectors

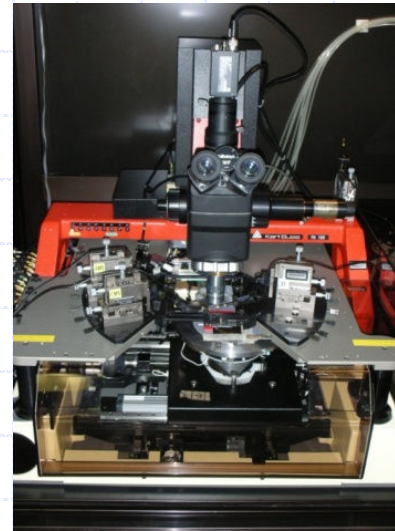
Prototype detectors: double sided silicon strip, manufactured by ITC-Fondazione Bruno Kessler  
active area =  $3 \times 3 \text{ cm}^2$   
strip pitch =  $500 \text{ }\mu\text{m}$   
strip width =  $300 \text{ }\mu\text{m}$  and  $200 \text{ }\mu\text{m}$   
thicknesses =  $1 \text{ mm}$  ( $1.5 \text{ mm}$ )  
strip number = 64 orthogonal p and n strips on opposite sides



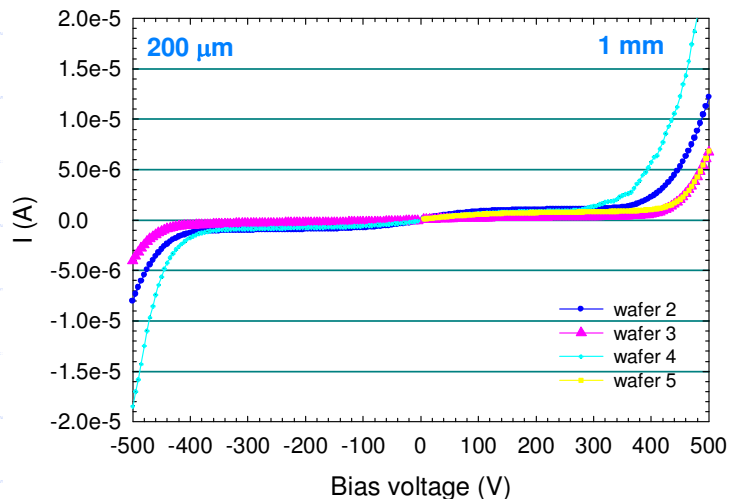
PCB support containing the sensor n-side bonded to a VaTaGP2.5 ASIC (Ideas)

# Electrical Characterization (I)

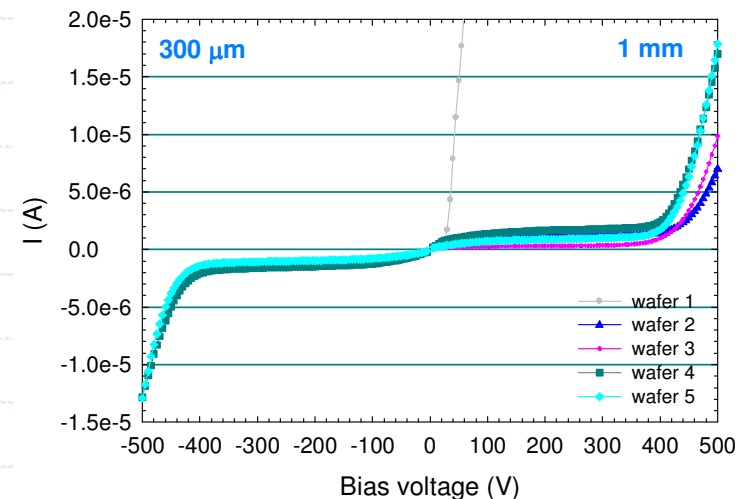
A reverse voltage ramp is applied on the n (p)-side bias line while measuring the current flowing at p (n)-side bias ring terminal kept at the ground potential. Bias-ring current includes the leakage current contribution of all strips.



Test-station for electrical characterization of the sensors.



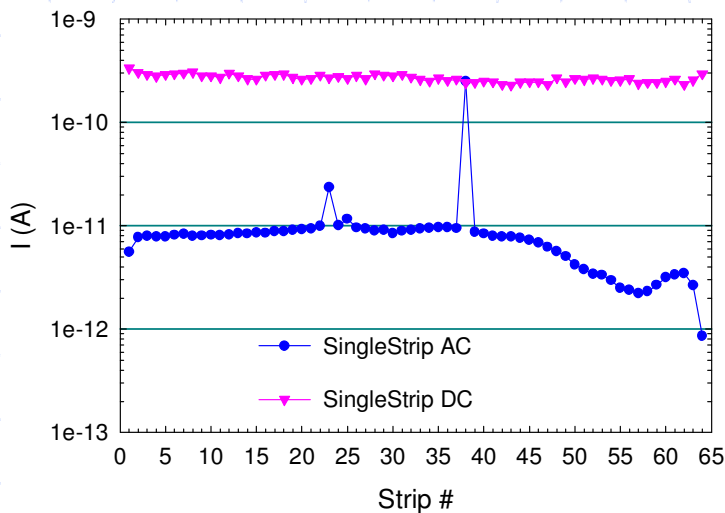
Total leakage currents of some tested detectors.



# Electrical Characterization (II)

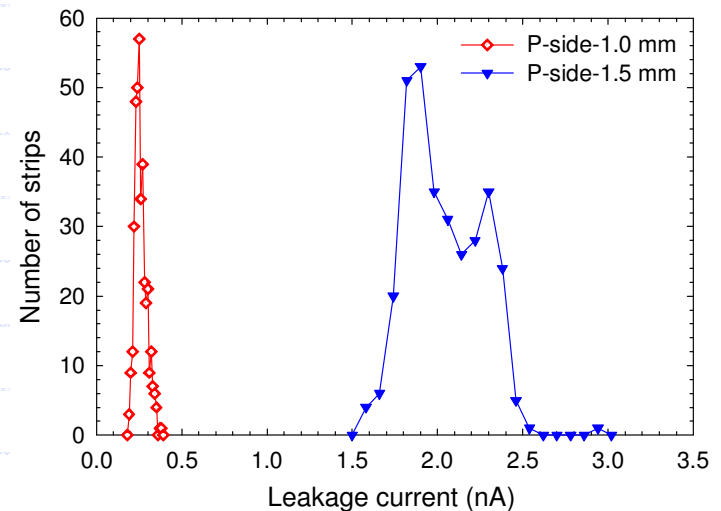
DC scans: no defective strips.

AC scans present a negligible number of broken capacitors (~4%).



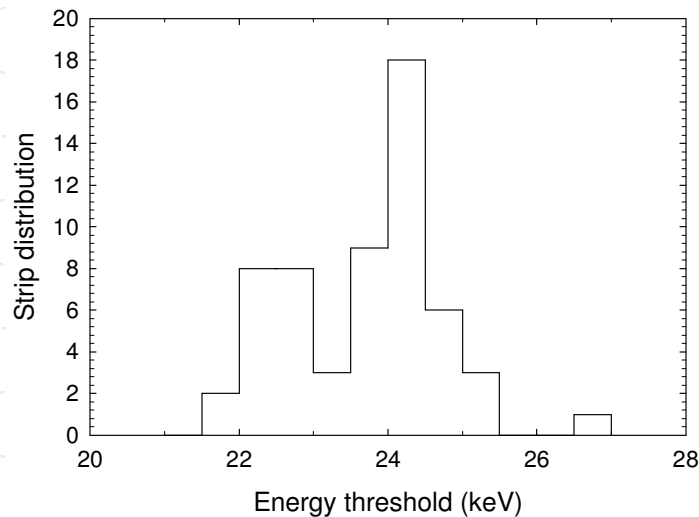
Typical example of a DC and AC scan of the p-side. We can note the broken capacitors.

Distributions of the single strip DC currents of the p-sides: two distinct groups of strips having different leakage current values can be observed, corresponding to the two different detector thicknesses, 1.0 and 1.5 mm.



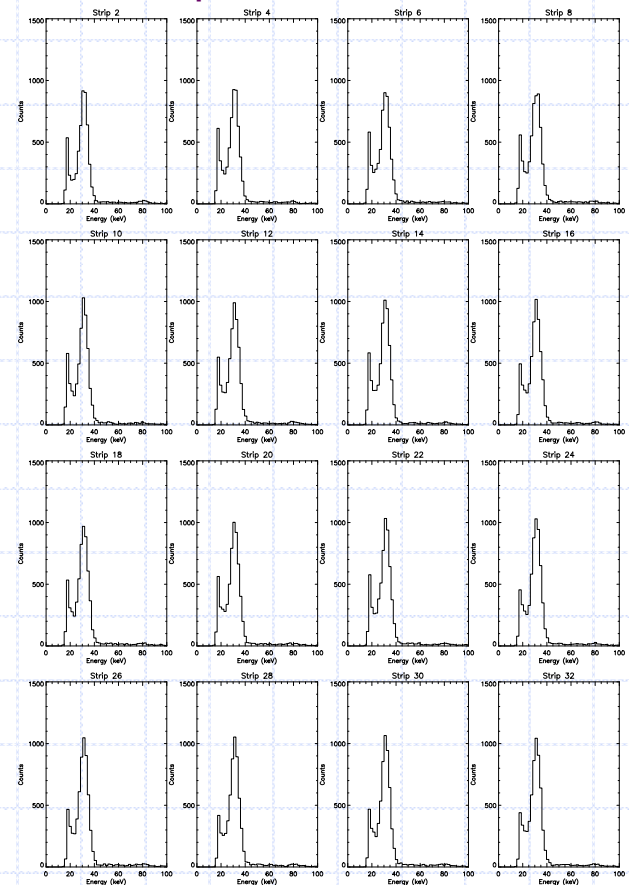
# Spectroscopic Characterization

Distribution of the low energy threshold values measured for a sensor evaluating the minimum energy relievable in the strip spectra of a  $^{133}\text{Ba}$  source.



**Low energy threshold: ~25 keV.**

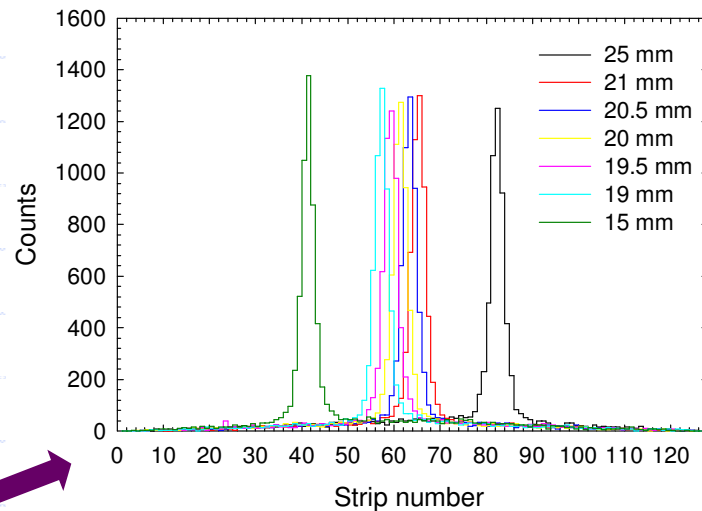
Example of 16 spectra acquired with  $^{133}\text{Ba}$ .



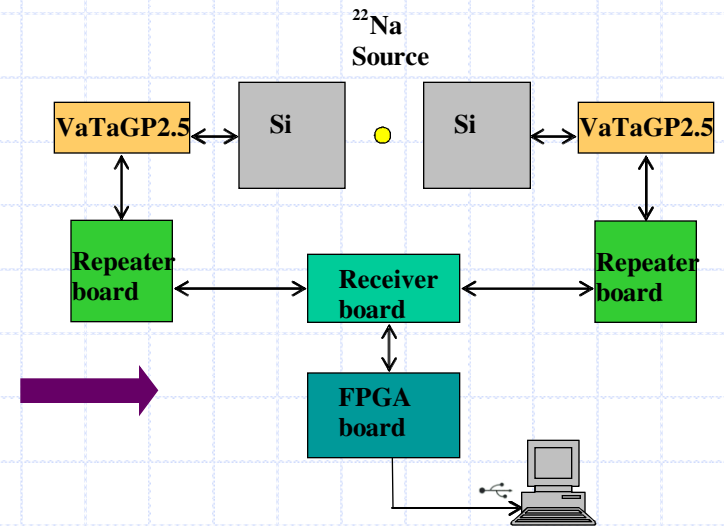
# Spatial resolution

Block diagram of the experimental setup: a  $^{22}\text{Na}$  spherical source was positioned between two opposed detectors in seven different positions.

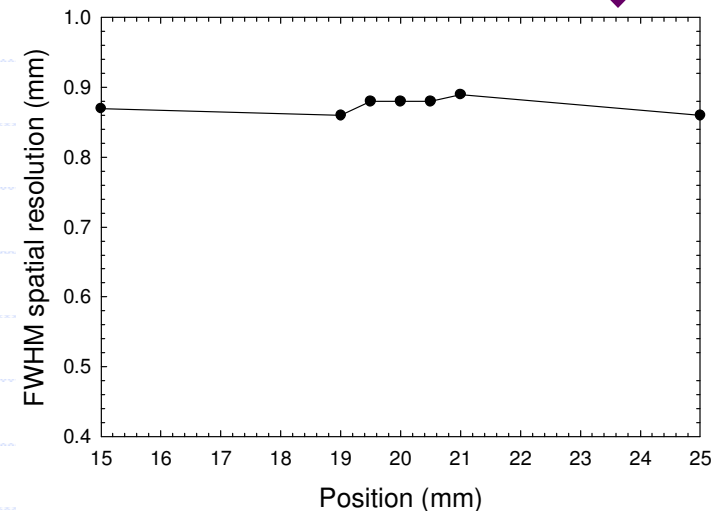
The source diameter is of  $\sim 1$  mm.



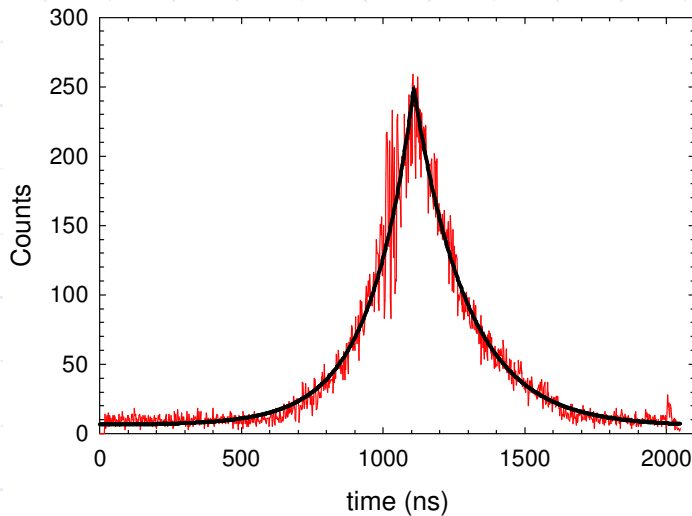
The profiles as a function of the source position on the silicon sensors at  $\pm 0.5$ , 1 and 5 mm, with respect to a central strip, in the orthogonal direction to the strips.



The average FWHM: 0.87 mm  
The detector intrinsic spatial resolution: 0.51 mm.



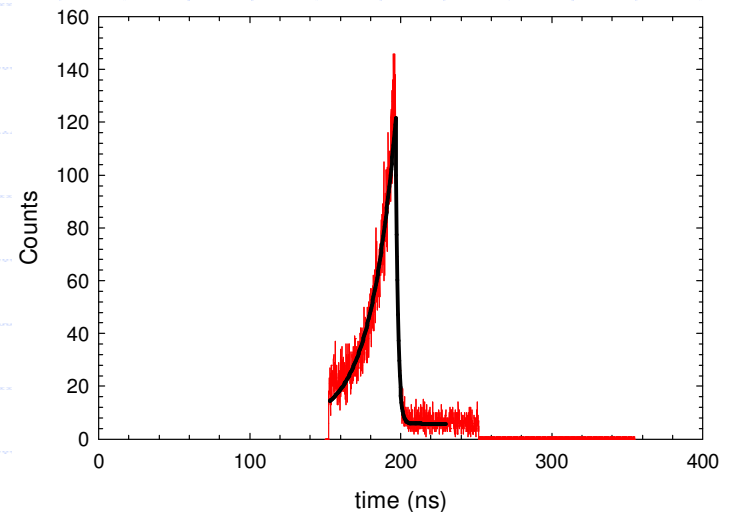
# Coincidence Timing resolution (I)



Timing spectrum acquired using a  $^{22}\text{Na}$  radioactive source between two opposed silicon detectors.

The estimated timing resolution (FWHM):  
~200 ns (due to the amplitude walk).

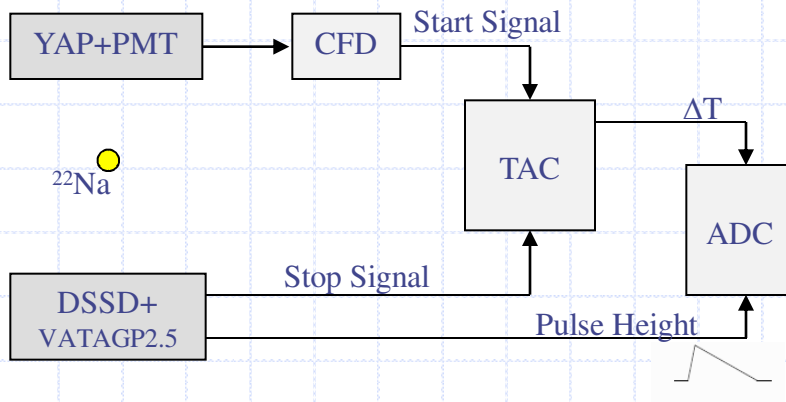
Using a dedicated ASIC designed by the Politecnico of Milano for fast timing measurements we have obtained an improved resolution of 16.5 ns (FWHM). This was measured using a  $^{22}\text{Na}$  radioactive source placed between a silicon detector and a YAP detector optically glued to a PMT with constant fraction timing.





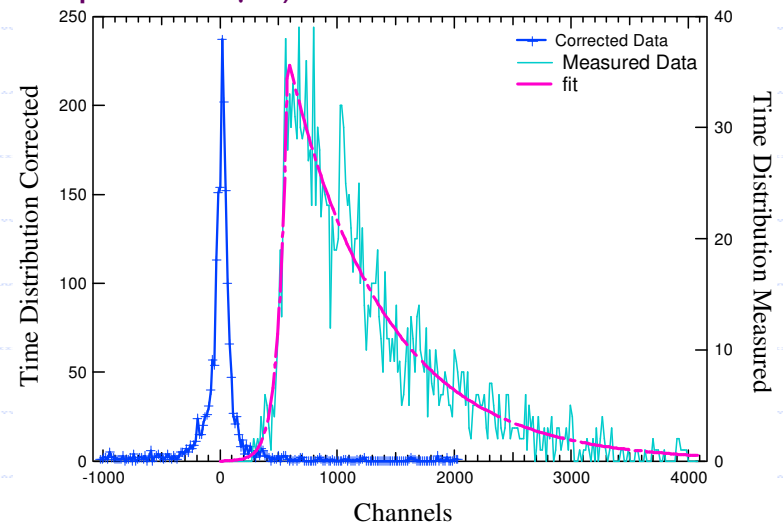
# Coincidence Timing resolution (II)

The amplitude walk correction method requires the acquisition of the timing signal and the pulse height for each event. The time resolution before correcting was  $128 \pm 3$  ns, while after compensating it is  $18 \pm 3$  ns.



Comparison between the data before and after correction.

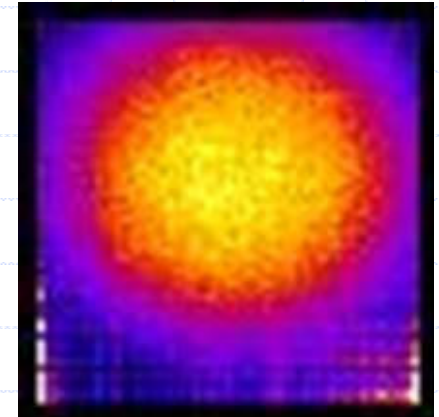
Block diagram of the experimental setup used for compensating the timing measurements carried out with a Double Sided Silicon Detector coupled to a VATAGP2.5 ASIC (peaking time of fast shaper  $\rightarrow 1 \mu\text{s}$ ).





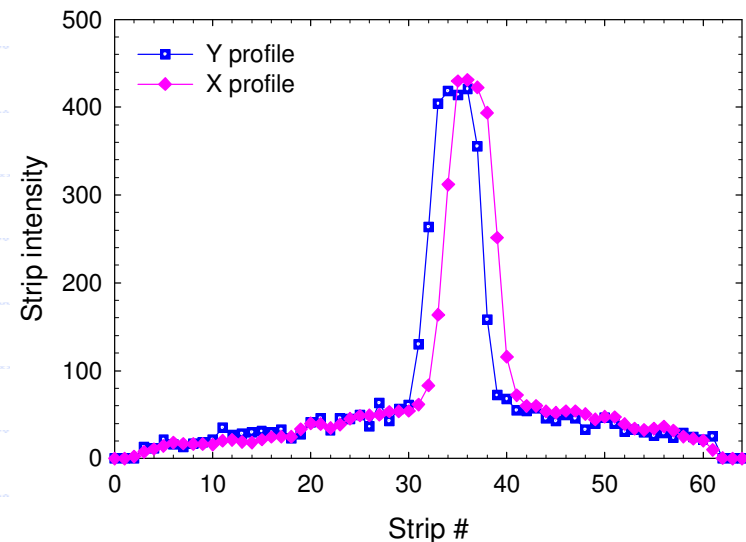
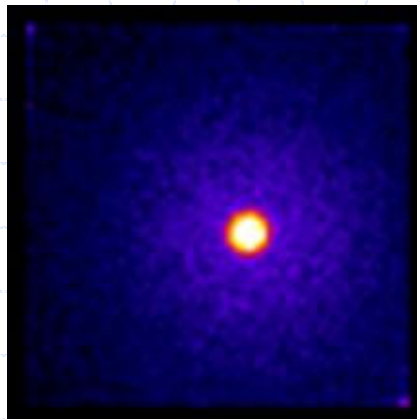
# Imaging Performance (I)

Response uniformity obtained irradiating the whole detector with an uncollimated source of  $^{57}\text{Co}$ .



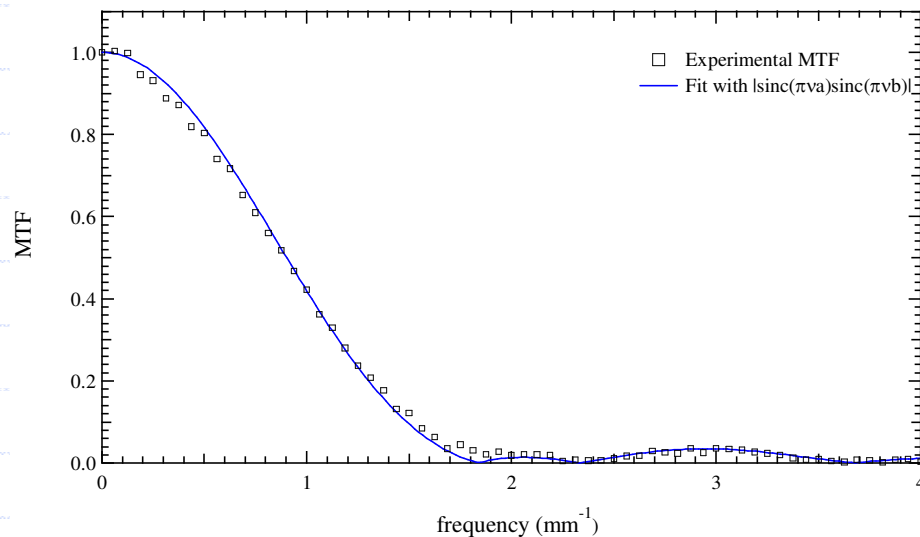
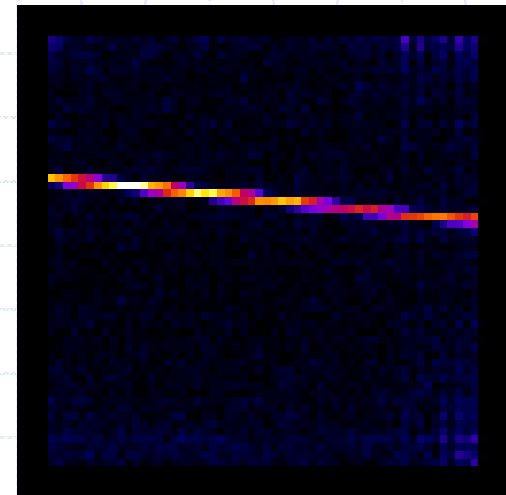
2-D image (left) obtained by illuminating the detector with a collimated  $^{57}\text{Co}$  source.

The collimator hole has a diameter of 1.5 mm and the calculated spot on the detector is 3 mm corresponding to 6 strips in agreement with the X and Y profiles (right).



# Imaging Performance (II)

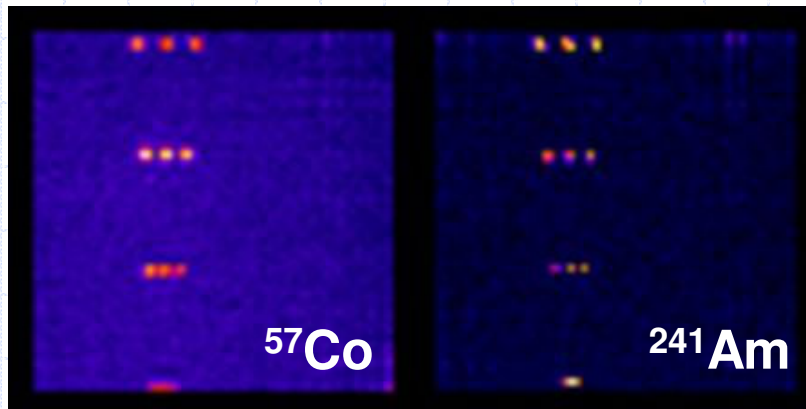
2-D image acquired irradiating a sensor with a  $^{241}\text{Am}$  source through a 0.35 mm slit in order to calculate the modulation transfer function.



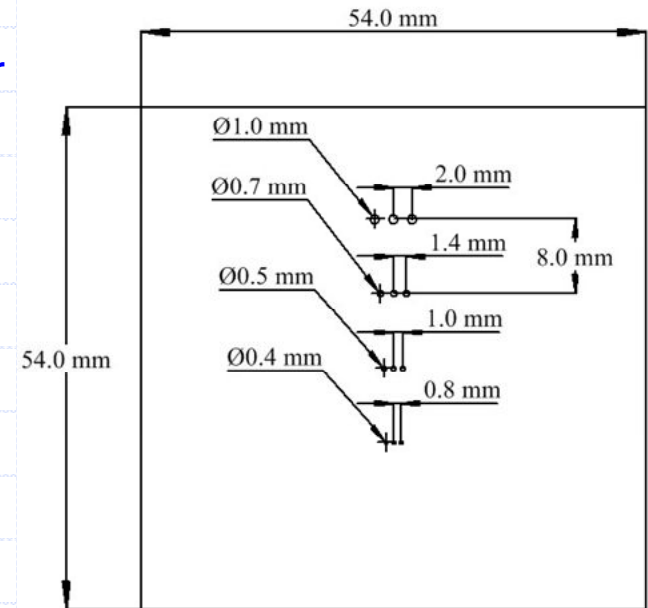
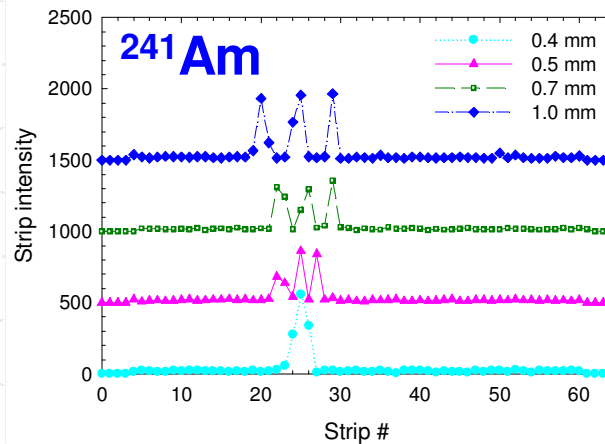
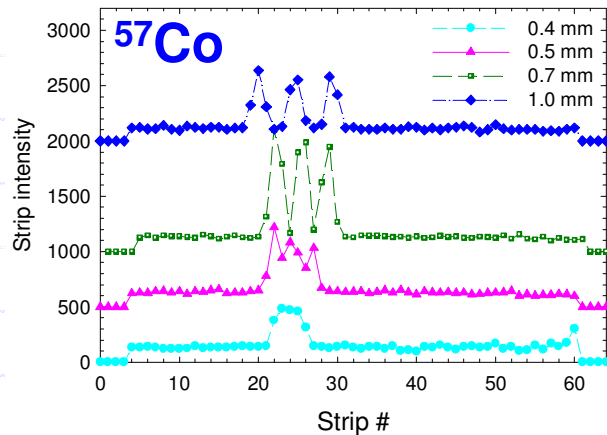
Slit width =  $(0.43 \pm 0.03)$  mm  
Strip pitch =  $(0.54 \pm 0.04)$  mm

# Imaging Performance (III)

2-D images acquired by illuminating the sensor through a Pb mask with  $^{57}\text{Co}$  and  $^{241}\text{Am}$ .



Horizontal profiles



We can conclude that the spatial resolution of the detector is dominated by the strip pitch.

# Conclusions

- ✓ Our simulations have shown the good performance of a small animal PET scanner based on thick double-sided silicon detectors
- ✓ Proof of principle measurements have confirmed the expected very high spatial resolution
- ✓ Energy threshold  $\leq 28$  keV (required  $\leq 50$  keV)
- ✓ Intrinsic spatial resolution  $< 0.6$  mm
- ✓ Timing resolution  $\approx 20$  ns FWHM using either a dedicated ASIC designed by the Politecnico of Milano for fast timing measurements or amplitude walk correction methods

## Future developments

- ✓ We have developed a very compact readout electronics based on VATAGP7.1 ASIC (nominal peaking time of fast shaper  $\rightarrow 50$  ns), to reduce the time walk variations.

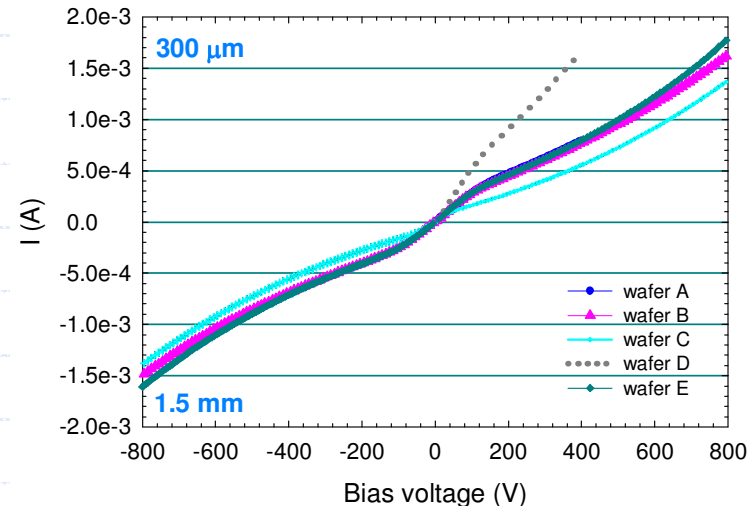
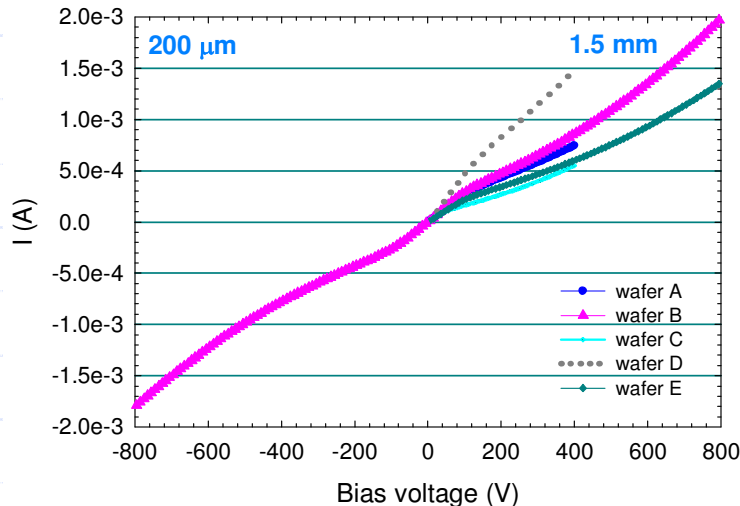
# Introduction

Positron Emission Tomography (PET) requires the determination of lines of flight (LOFs) of the two (almost) back to back 511keV gamma rays generated by a  $e^+ e^-$  annihilations.

The positron emitted from a  $\beta^+$  decay will thermalise, after having traveled a certain distance (typically referred to as ***positron range***), and then annihilate with an electron. In most annihilations 2 gammas will be emitted each carrying away 511 keV. There is an angular dispersion from collinearity of about  $0.5^\circ$  due to the Fermi motion of the  $e^+e^-$  center of mass. This is typically referred to as the ***non collinearity*** of the emitted gamma rays.

# Electrical Characterization (III)

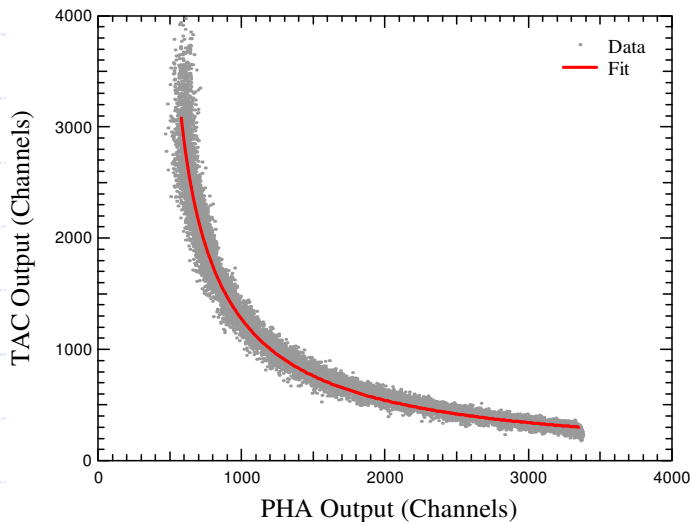
A reverse voltage ramp is applied on the n (p)-side bias line while measuring the current flowing at p (n)-side bias ring terminal kept at the ground potential. Bias-ring current includes the leakage current contribution of all strips.



# Amplitude walk correction method

An initial calibration was carried out injecting an increasing test pulse into the preamplifier input of a channel through a  $\sim 1$  pF internal capacitor, the same test pulse provides the start signal to the TAC unit, while the stop signal is the trigger signal generated by the VATAGP2.5 ASIC. The time delays measured by the TAC unit are sampled in coincidence with the corresponding analog signals. The following plot reports the TAC output as a function of the recorded pulse height amplitude. The data were fitted with the function that expresses the shaper output signal dependence on time represented by the black solid line:

$$E(t) = E \cdot \left(\frac{t}{\tau}\right)^n \cdot e^{-\frac{t}{\tau}} \quad \text{where } t \text{ is the time constant and } E \text{ is the amplitude at } t=0.$$



Starting by the parameters calculated with the calibration data fit we have determined the mean delay corresponding to each pulse amplitude and afterwards we have recorded the time spectrum employing the experimental set up of the previous figure where the timing signal is acquired in coincidence with the recorded pulse height for each event coming from a double sided silicon detector read by a VATAGP2.5 ASIC. Each pulse amplitude, coming from the silicon detector, was corrected subtracting the time delay obtained by calibration data fit from the measured delay  $\Delta T$ . The time resolution (FWHM) before correcting was  $128 \pm 3$  ns, while after compensating it is  $(18 \pm 3)$  ns.



# VATAGP2.5 ASIC

The VATAGP2.5 is a 128-channels “general purpose” charge sensitive amplifier: each channel is composed of a low-noise/low-power preamplifier, a shaper (peaking time of 3.1  $\mu\text{s}$ ) with sample/hold, multiplexed analogue readout and a fast shaper (peaking time of 1.1  $\mu\text{s}$ ) that gives a trigger signal.

The ASIC provides 3 modes for multi-channel readout:

- 1) serial readout all channels: the analog values from all channels can be read sequentially;
- 2) sparse readout: the channel that is triggered is stored in a buffer and only the hit channel signal is available; this allows the analog values and addresses from only the channels that triggered to be read;
- 3) sparse with neighbour channels readout: the user supplies an address, and reads the analog value of that channel and of the adjacent channels.

Each discriminator can be disabled and the channel threshold can be adjusted using a 5-bit global threshold DAC and individually using a 4 -bit DAC.

Each channel can be individually tested by injecting a test charge into the preamplifier input of the channel that has been selected. With this feature we tested the chips without connecting the detector.

The results of the ASIC functional characterization are:

- the dynamic range was measured to cover from  $-11 \text{ fC}$  to  $7.5 \text{ fC}$  with good linearity;
- the chip output saturates at about  $24 \text{ fC}$  for positive signal;
- the channel to channel gain dispersion is  $\sim 10\%$ ;
- the gaussian fit of the distribution of noise values for the bonded channels gives a spread  $s$  of  $0.6 \text{ mV}$  corresponding to  $34.3 \text{ e}^-$ ;
- the time jitter is  $\sim 15 \text{ ns FWHM}$  from  $220$  to  $511 \text{ keV}$  and increases for energies lower than  $220 \text{ keV}$ .

# Multiple interactions

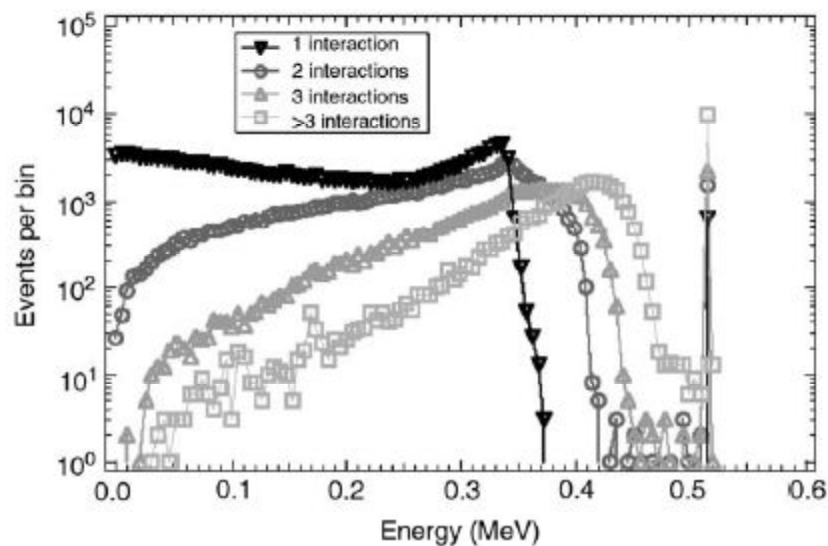


Fig. 1. Energy deposit for 511 keV gamma rays as a function of the number of interactions in a 4 cm thick slab of Silicon. The abscissa represents the energy, in MeV, deposited in the Silicon. The narrow peak at 511 keV are full energy events. Most full energy peaks are for events with more than three interactions.